Journal of Materials Chemistry A

Accepted Manuscript

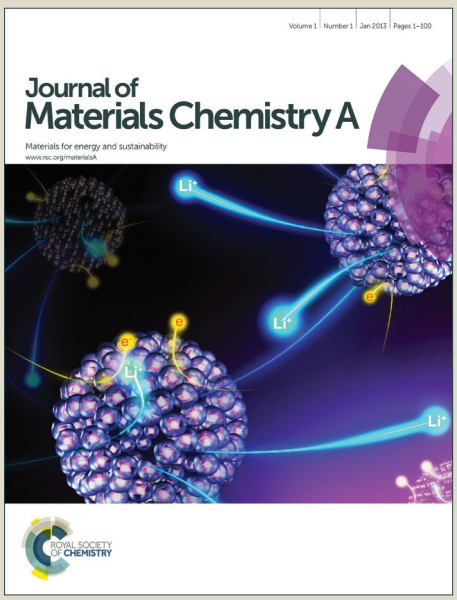

ROYAL SOCIETY OF CHEMISTRY

www.rsc.org/materialsA

Journal Name

RSCPublishing

ARTICLE

In situ cross-linked superwetting nanofibrous membranes for ultrafast oil/water separation

Cite this: DOI: 10.1039/x0xx00000x

Aikifa Raza,[a] Bin Ding,[*a,b] Ghazala Zainab,[a] Mohamed. El-Newehy,[c,d] Salem S. Al-Deyab, [*c] and Jianyong Yu[b]

Received 00th January 2012,
Accepted 00th January 2012

DOI: 10.1039/x0xx00000x

www.rsc.org/

Creating a practical and energy-efficient method with high efficacy to separate oil/water mixtures, especially those stabilized by surfactants has proven to be extremely challenging. To cope with these challenges, a novel and scalable strategy was developed for the synthesis of superhydrophilic and prewetted oleophobic nanofibrous membranes by the facile combination of *in situ* cross-linked polyethylene glycol diacrylate nanofibers supported on polyacrylonitrile/polyethylene glycol nanofibrous (x-PEGDA@PG NF) membranes. The as-prepared x-PEGDA@PG NF membranes have shown superhydrophilicity with ultralow time of wetting and promising oleophobicity to achieve effective separation for both immiscible oil/water mixtures and oil-in-water microemulsions solely driven by gravity. These new membranes having good mechanical strength of 14 MPa and mean pore size between 1.5-2.6 μm have shown very high flux rate of 10,975 L m^{-2} h^{-1} with extremely high separation efficiency (residual oil content in filtrate is 26 ppm). More importantly, the membrane exhibits high separation capacity, which can separate 10 L of an oil/water mixture continuously without a decline in flux and excellent antifouling property for long term use. Thus making them an important candidate for treating wastewater produced in industry and daily life, crude oil, especially for high viscosity oil purification.

Introduction

In the last decade, increased oily wastewater due to rapid industrialization in global cities and multiple oil spill disasters within the marine ecosystems have highlighted the challenges of effective oil/water, especially the oil/water micro- and nano-emulsions separation.[1, 2] Clean-up and recovery from an oil spill is difficult and depends upon many factors, including the type of oil spilled, the temperature of the water (affecting evaporation and biodegradation), and the types of shorelines and beaches involved.[3] Conventional methods for cleaning up such as, bioremediation, controlled burning, dispersants, air flotation, skimming, oil-absorbing materials, and flocculation are limited by low separation efficiency, energy-cost, and complex separation instruments, and also not much effective for separating surfactant-stabilized microemulsions with a dispersed droplet size below 20 μm.[4-8]

Diverse interfacial effects of oil and water towards the surfaces and by utilizing the superwetting behaviour of solid surfaces to design an oil/water separation process is considered an effective method.[9-11] A series of superwetting materials along with polymer based filtration membranes were also employed for the separation of surfactant-stabilized oil-in-water emulsions driven by external pressure.[12-14] But the most serious limitation of these type of membranes is the low flux and quick decline of permeation due to oil adsorption and/fouling issues which are harder to clean. In addition, these selectively wettable materials are not applicable for emulsified oil/water separation because the pore sizes in these materials (>50 μm) are much larger than the droplet sizes of the emulsion (<20 μm).[15] In last decade, superhydrophobic/superoleophilic materials in combination with surface chemistry and roughness have been broadly investigated and used to remove oils from water.[16, 17] Water being denser than oils tends to form a barrier layer to prevent oil permeation and creates fouling problems. Consequently, superhydrophobic materials are unsuitable for the separation of water rich oil/water mixtures or oil-in-water emulsions.[18]

Practically, developing superhydrophilic and oleophobic surfaces may provide an alternative and feasible way for oil/water separation, but due to the higher surface tension of water than oil, the oleophobic surfaces are also hydrophobic.[19] The most effective way to achieve oleophobicity is by introducing fluorinated low surface energy materials on micro/nano-hierarchical structures.[20-23] Besides the environmental hazards, the fluorinated oleophobic surfaces are only stable in air, and lose their oleophobicity in water.[24-26]

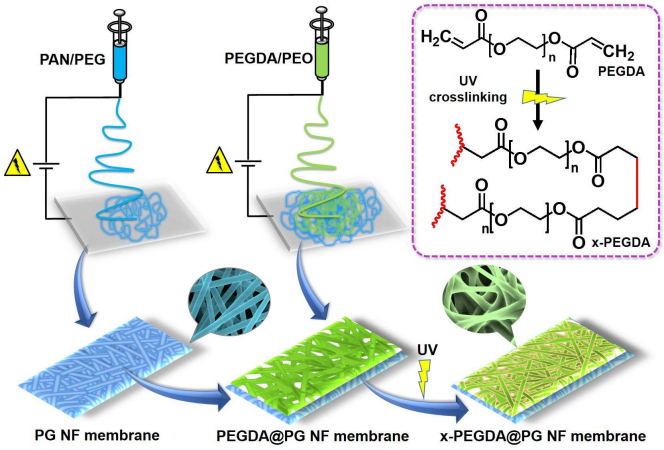

Scheme 1 Schematic illustration of in situ cross linking approach for the fabrication of x-PEGDA@PG NF membranes.

Recently, by taking advantage of high energy materials with superhydrophilicity to construct oleophobic prewetted surfaces with oil/water/solid three-phase systems were proposed. Following this strategy, oleophobic surfaces could be easily achieved in water by a simple and fluoride-free way. By combining the simplicity and strength of electrospinning method with right type of material, the functional fibrous membranes at nano- and microscale levels could be fabricated.[27-30] Superhydrophobic electrospun fibrous membranes including polystyrene, polyvinylidene fluoride, poly(methyl methacrylate), and polyurethane have already been fabricated.[15, 31-33] Also reported is the preparation of electrospun porous polystyrene membranes for oil adsorption.[34-36]

However, the fabrication of high surface energy fibrous membranes and prewetted oleophobic characteristics with a high separation efficiency and large separation capacity is still ambiguous and highly required.[37-39] In this contribution, we present the fabrication of superwetting superhydrophilic and prewetted oleophobic nanofibrous (NF) membranes by the combination of *in situ* cross-linked functional NF layer of polyethylene glycol diacrylate (PEGDA) deposited over polyacrylonitrile/polyethylene glycol (PG NF) membrane, as shown in Scheme 1. Key to our development design is that the use of x-PEGDA NF layer has not only amplified the superhydrophilicity of PG NF membrane, but also endowed the required oleophobicity to the prewetted NF membranes. Which is capable of providing an effective gravity driven separation for both oil/water mixture and oil-in-water emulsion with ultrafast flux rate and very high separation efficiency.

Experimental

Materials

Polyacrylonitrile (PAN, M_w=90, 000) was purchased from Kaneka Co., Ltd., Japan. PEGDA, polyethylene oxide (PEO) (M_w=60, 000), 1-hydroxycyclohexyl phenyl ketone (HCPK), sodium dodecyl sulphate (SDS), and oil red were purchased from Aladdin Chemistry Co. Ltd., Shanghai, China. Polyethylene glycol (PEG) (M_w=2000), was purchased from Sinopharm Chemical Reagent Co. Ltd. *N*,*N*-dimethylformamide (DMF), dichloromethane, and hexane were supplied by Shanghai Chemical Co., China. All chemicals were of analytical grade and were used without further purification.

Fabrication of PG NF membranes

PAN/PEG (8/0, 8/2, 10/2, and 12/2 w/w) solutions were prepared by dissolving in DMF with stirring for 24 h. The electrospinning process was performed using the DXES-1 spinning equipment (Shanghai Oriental Flying Nanotechnology Co., Ltd., China). Firstly, the PAN/PEG solutions was loaded into a syringe and injected through a metal needle with a controllable feed rate of 1 mL/h. A high voltage of 20 kV was applied to the needle tip, resulting in the generation of a continuous jet stream. The resultant fibrous membranes were deposited on woven polyester (PET), non-woven polypropylene (PP), and aluminium foil covered grounded metallic rotating roller at a 15 cm tip-to collector distance, and then dried in vacuum at 80 ^{o}C for 2 h. The obtained membranes from various concentrations (x wt%) of PAN with and without PEG were denoted as PAN-x and PG-x NF membranes.

Fabrication of x-PEGDA@PG NF membranes

The solutions of PEGDA/PEO/HCPK (10/3/1 w/w/w) were prepared in water with continuous stirring for 6h. The above PG-x NF membranes were used as substrate to deposit PEGDA/PEO nanofibers, using high voltage of 20 kV with controllable feed rate of 1 mL/h at a 15 cm tip-to collector distance. The as deposited membranes were cross-linked for 30 sec using a UVP XX-40S ultra violet bench lamp (wavelength, 254 nm), and were denoted as x-PEGDA@PG-x NF membranes.

Oil/water separation experiment

Oil/water mixture and oil-in-water emulsion were used for separation experiment. Oil/water mixtures were prepared by mixing water and sunflower oil with the weight ratio 9:1 v/v. For convenience oil was dyed red using oil red. Oil-in-water emulsions were prepared by mixing water and sunflower oil in a ratio of 9:1 v/v with 0.1 mg of SDS per ml of emulsion. And was sonicated under a power of 2 kW for 2 h to produce a white and milky solution. Other low and high density oil/water [hexane/water (H/W), petrol/water (P/W), crude oil/water (Co/W, soybean oil/water (S/W), and dichloromethane/water (D/W)] mixtures were also used for separation experiments. Commonly, the obtained emulsions could be stable for 30 min when stored under ambient conditions. The droplet size of oil-in-water emulsions are in the range of 5-40 μm as observed by optical microscopy. The as-prepared NF membrane was fixed between two glass vessels with a diameter of 39 mm. The above oil/water mixtures and oil-in-water emulsions were poured into the membranes and the separation was achieved solely driven by gravity.

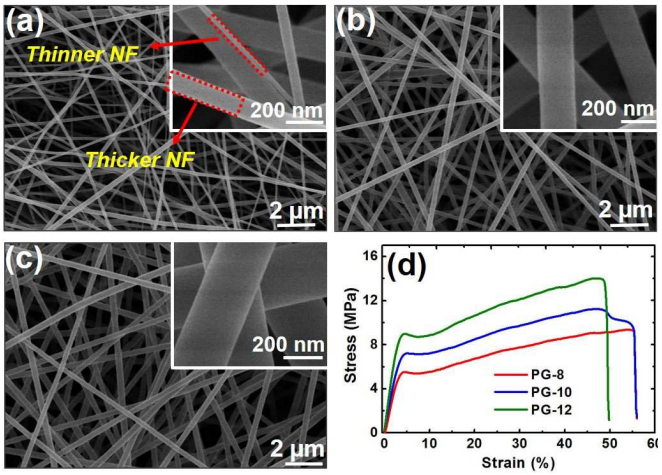

Fig. 1 FE-SEM images of (a) PG-8, (b) PG-10, and (c) PG-12 NF membranes. (d) Stress-strain curve for the relevant PG-8, PG-10, and PG-12 NF membranes.

The filtrate water was collected and the residual oil content in the filtrate was calculated by measuring chemical oxygen demand (COD) in the water (detailed procedure in supporting information).

Characterization

The morphology of membrane was examined by a field emission scanning electron microscope (FE-SEM) (S-4800, Hitachi Ltd. Japan). FT-IR spectrograph was carried out by a Nicolet 8700 FT-IR spectrometer. The mechanical properties of the membranes were performed on a tensile tester (XQ-1C, Shanghai New Fiber Instrument Co., Ltd., China). The porous structure was characterized using a capillary flow porometer (CFP-1100AI, Porous Materials Inc., USA). Water contact angle (WCA) (3 μL) and oil contact angle (OCA) (3 μL) measurements were performed using a contact angle goniometer Kino SL200B equipped with tilting base.

Results and discussion

Owing to the different interfacial properties of oil and water, the design of NF membranes requires dual wetting behaviour (robust superhydrophilicity and oleophobicity) with comparable mechanical strength for an effective oil/water separation process. The representative FE-SEM image of NF membranes obtained by varying the concentrations of PAN (8, 10, and 12) with fix concentration of PEG (2 wt%) revealed a randomly oriented 3D nonwoven structure (Fig. 1a-c). As shown in Fig. 1a, PG-8 NF membranes exhibited thinner (average diameter of 63 nm) and comparatively thicker (average diameter of 128 nm) nanofibers (indicated by red dotted lines) without any adhesion among the adjacent nanofibers. The formation of these fibers could be attributed to the presence of small amount of PEG in the electrospinning solution.[40] Because at higher concentrations (PG-10 and PG-12) the content of PEG decreases with respect to PAN concentration and thus uniform NF morphology with increased average fibrous diameter of 157 and 228 nm was obtained (Fig. 1b,c).

The addition of low molecular weight PEG to the PAN electrospinning solution has improved the mechanical strength of resultant PG-x NF membranes by improving the packing density of the resultant membranes.[41, 42] Fig. 1d present the typical stress-strain curve of relevant PG-x NF membranes, exhibiting a typical nonbonding structure. It showed a linear elastic behaviour in the first region under a stress load until reaching to the yield point, and then curves presented a nonlinear elastic behaviour until break due to the slip and "pull out" process of the individual PG-x NF along the stress direction.[42-44] The relevant membranes of PG-8, PG-10, and PG-12 possessed the robust tensile strength of 9.36, 11.24, and 14.01 MPa, respectively, indicating a regular increase of tensile strength with increasing the concentration. This is likely due to an increased friction force between PG fibers and the enhanced electrospinnability with increasing concentration of PAN solutions.

To improve the water permeability and to decrease the fouling (oleophilicity), PG-8, PG-10, and PG-12 NF membranes were further top coated by electrospun fibers of PEGDA/PEO.

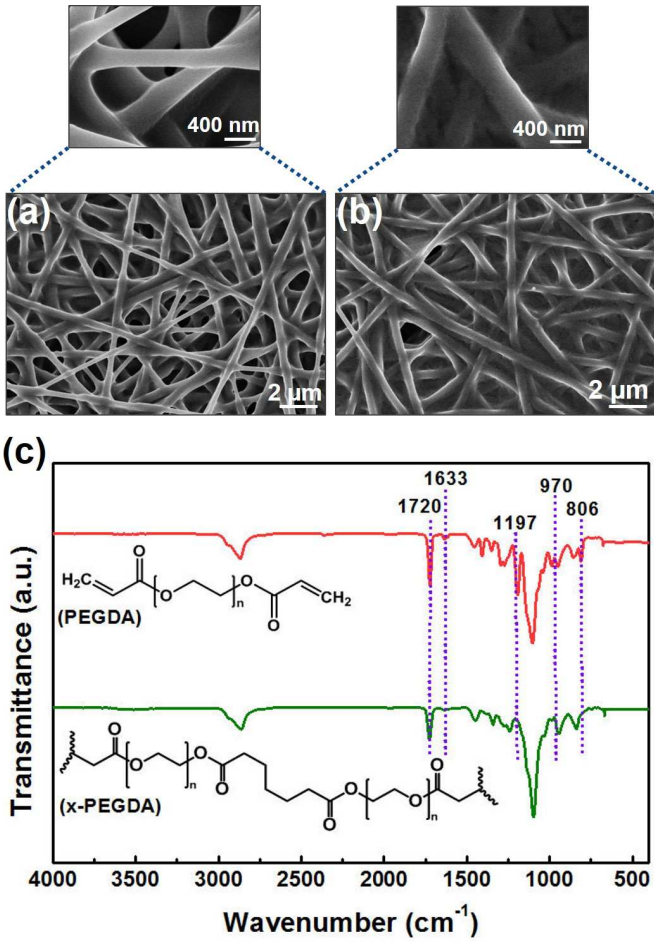

Fig. 2 FE-SEM images of (a) PEGDA@PG-8 and (b) x-PEGDA@PG-8 NF membranes at low and high resolution. (c) FT-IR spectrum of PEGDA and x-PEGDA NF membranes.

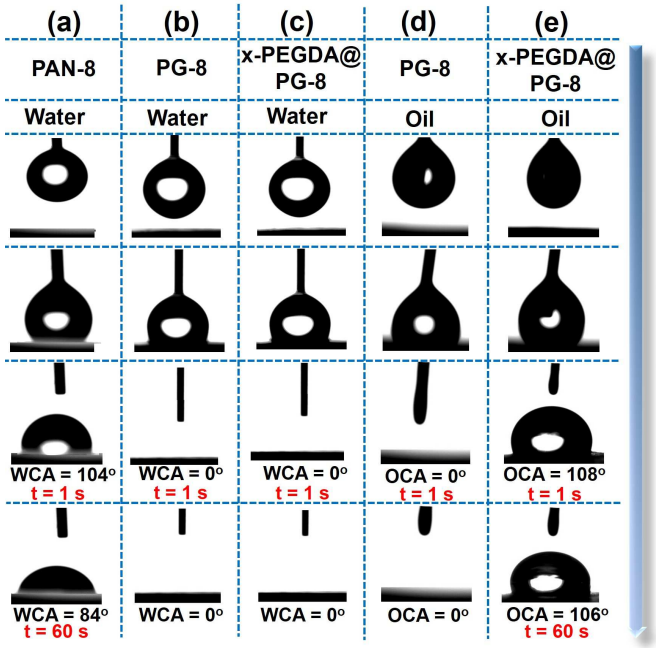

Fig. 3 Optical snapshots of dynamic contacting processes of water droplets onto (a) PAN-8, (b) PG-8, and (c) x-PEGDA@PG-8 and oil droplets onto (d) PG-8 and (e) x-PEGDA@PG-8 NF membranes.

Fig. 2a,b present the FE-SEM image of top surface of PEGDA@PG-8 and cross-linked x-PEGDA@PG-8 NF membranes. PEGDA@PG-8 NF membranes have shown the randomly oriented three-dimensional nonwoven structures (average diameter of 313 nm), with prominent adhesion among the adjacent nanofibers. Which could be attributed to the incomplete solvent (water) evaporation that has good solubility for both PEGDA and PEO. Fig. 2b has shown increased fibrous diameter (377 nm) with more filled gaps among the adjacent fibers to confirm the accomplishment of *in situ* cross-linking of PEGDA/PEO fibers deposited at various PG-x NF membranes. The mechanical behaviour and crosslinking reaction of x-PEGDA@PG NF membranes is presented in supporting information. FT-IR spectrum further confirms the *in situ* cross-linking of PEGDA (Fig. 2c).[45-47] The bands appeared at 1633, 970, and 806 cm^{-1} are attributed to the double bonds of the acrylates (Fig. 2c, upper curve), while these peaks of double-bonds greatly reduced after *in situ* cross-linking (Fig. 2c, lower curve), which suggested that most of the □C=C□ bonds had been polymerized. The bands at 1720 and 1197 cm^{-1} were assigned to the C=O stretching and C□O asymmetric stretching vibration of group (□C□O□C□), respectively. After UV-irradiation the height of these peaks changed little, indicating that the inherent structures of PEGDA except □C=C□ bonds were not damaged.[48]

Presence of acrylonitrile and vinyl co-monomers in the skeletal chain of the PAN make it hydrophilic, thus leading to a high surface energy of larger than 40 mN m^{-1}.[40] The addition of extremely hydrophilic low molecular weight PEG to the PAN electrospinning solution has further augmented the hydrophilicity of resultant PG-x NF membranes.

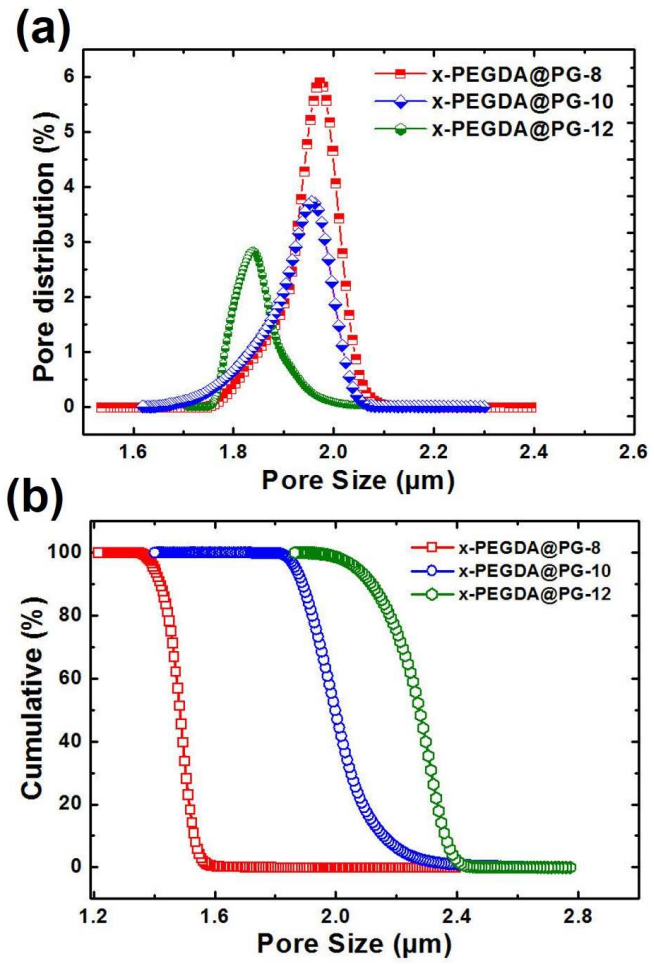

Fig. 4 Pore size distribution and cumulative porosity distribution curves of relevant x-PEGDA@PG-8, x-PEGDA@PG-10, and x-PEGDA@PG-12 NF membranes.

Fig. 3 showed the optical snapshots of dynamic contacting processes of water and oil droplets onto the surfaces of various membranes. As in Fig. 3a, the PAN-8 NF membrane has shown high time of wetting as compare to the PG-8 NF membrane, which has shown ultrafast spreading of water droplet on the surface (Fig. 3b). The nano structured fibrous architecture and extremely hydrophilic constituent of NF membrane promoted the water droplet spreading and permeating process by the capillary effect from nano-capillaries.[49, 50] Similar hydrophilic trend has been observed for the x-PEGDA@PG-8 NF membranes (Fig. 3c). For oleophobic characteristics, PAN-8 has shown superoleophilicity as oil immediately spread into the membrane (Fig. S5). For prewetted PG-8 the time of wetting of oil droplet is also very short, indicating the complete permeation of oil droplets on to the surface of NF membranes (Fig. 3d). On contrary, the prewetted x-PEGDA@PG-8 NF membrane has shown sufficient resistance towards the oil permeability with OCA of 106°, which could be attributed to the antifouling properties of cross-linked PEGDA molecules (Fig. 3e). Interestingly, very small decrease in OCA has been observed after 60 sec, thus proving x-PEGDA@PG-8 NF membranes with ultrafast superhydrophilic and pre-wetted

oleophobic characteristics for effective oil/water separation experiments. Although PG-8 NF membrane are also pre-wetted, but as water immediately permeated through the membranes, thus allowing the oil droplets to pass through the membrane presenting oleophilicity of the membrane. But in case of x-PEGDA@PG-8 NF membranes, the water not only immediately permeated thorough the membranes, but also retained within the interstitial spaces of *in-situ* cross-linked network of x-PEGDA. The pre-wetted oleophobic interface with low affinity for oil droplets prevents the as-prepared membranes from fouling by oils, which makes the recycling of oil easy.

The superhydrophilic and prewetted oleophobic property is attributed to the micro/nano-level hierarchical structures which are peculiar feature of electrospinning method and the superhydrophilic nature of *in situ* cross-linked x-PEGDA@PG NF membranes. When the as-prepared membrane is immersed in water, water could be trapped into the hierarchical structure to then form an oil/water/solid interface in the presence of oil.[51] The trapped water serves as a repulsive liquid phase for oils to contact with the NF membrane directly. For an oil/water/solid system with a rough surface, the contact angle could be expressed by the Cassie model as shown in equation (i):[52]

$$\cos\theta' = f\cos\theta + f - 1 \qquad \text{(i)}$$

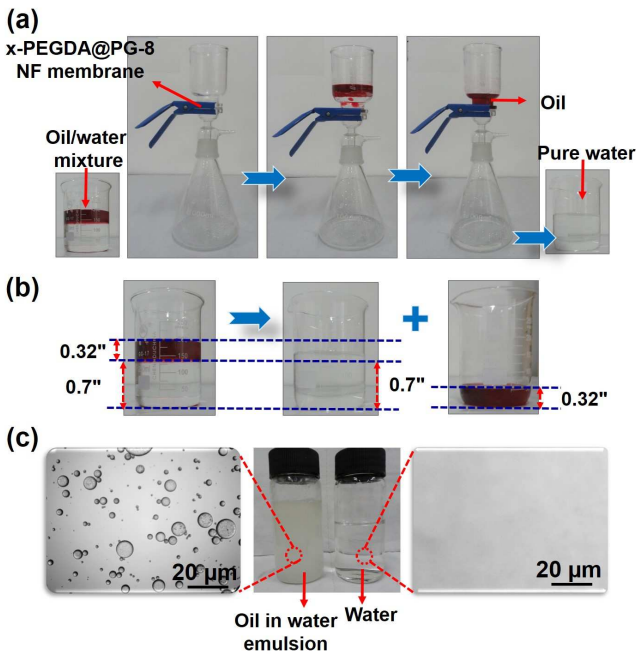

Fig. 5 The solely gravity-driven separation for oil water mixture using x-PEGDA@PG-8 NF membrane. For convenience oil was dyed red. (b) Photographs of oil water mixture (soybean oil) and water and oil collected after separation. (c) Photographs and optical micrographs of the oil/water emulsion before and after separation.

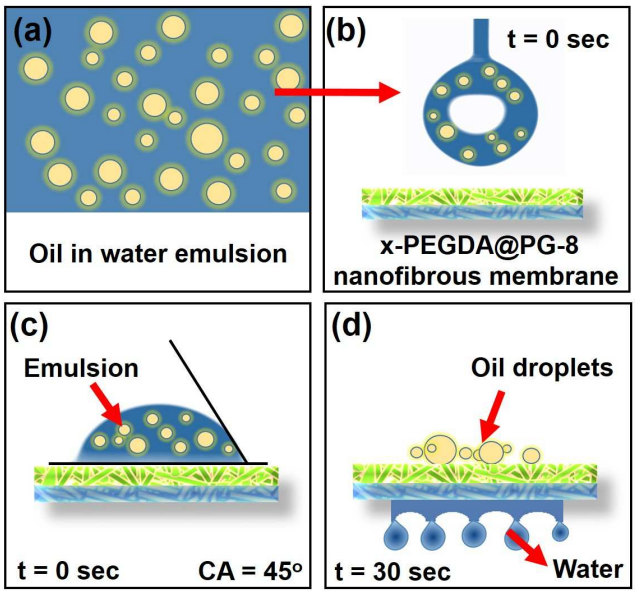

Fig. 6 Schematic illustration of separation characteristics of oil in water emulsion by using x-PEGDA@PG-8 NF membrane. (a) Mono-disperse oil in water emulsion, (b) emulsion droplet approaching the x-PEGDA@PG-8 NF membrane, (c) static contact angle of emulsion to the x-PEGDA@PG-8 NF membrane, and (d) schematic of dynamic oil water separation.

Where f, is the area fraction of the solid, θ is the contact angle of the oil droplet on a smooth surface in water, and θ' is the contact angle of the oil droplet on a rough surface in water. A smaller area fraction means a lower chance of the oil droplet contacting the solid surface, and the larger the oil CA θ' in water. The as-prepared x-PEGDA@PG NF membranes has a very rough surface, which implies a rather small area fraction of solid and a large oil contact angle (Fig. 3e).

The pore size, pore size distribution, and porosity of NF membranes are important parameters which should be considered for effective oil/water separation.[53, 54] The rupturing tendency of harden jet surface prior to drying of fibers in electrospinning process played an important role for the development of micropores in the fibers. Fig. 4a represent the typical pore size distribution of x-PEGDA@PG-8, x-PEGDA@PG-10, and x-PEGDA@PG-12 NF membranes measured through a capillary flow porometer. It is worth noting that the pore sizes of all the NF membranes were in the range of 1.5-2.4 µm. The mean flow pore size and the porosity of the relevant membrane are tabulated in the Table S1.

The decrease in the porosity is revealed with increase of NF diameter, and the maximum porosity value for the x-PEGDA@PG-8 NF membrane is representing the low tortuosity which is an indicator of geometry and interconnectivity of the pores.[54] Moreover, the cumulative pore size distributions (Fig. 4b.) of x-PEGDA@PG-8, x-PEGDA@PG-10, and x-PEGDA@PG-12 NF membranes presented that most of the pores are concentrated between 1.6 to 2.4 µm.

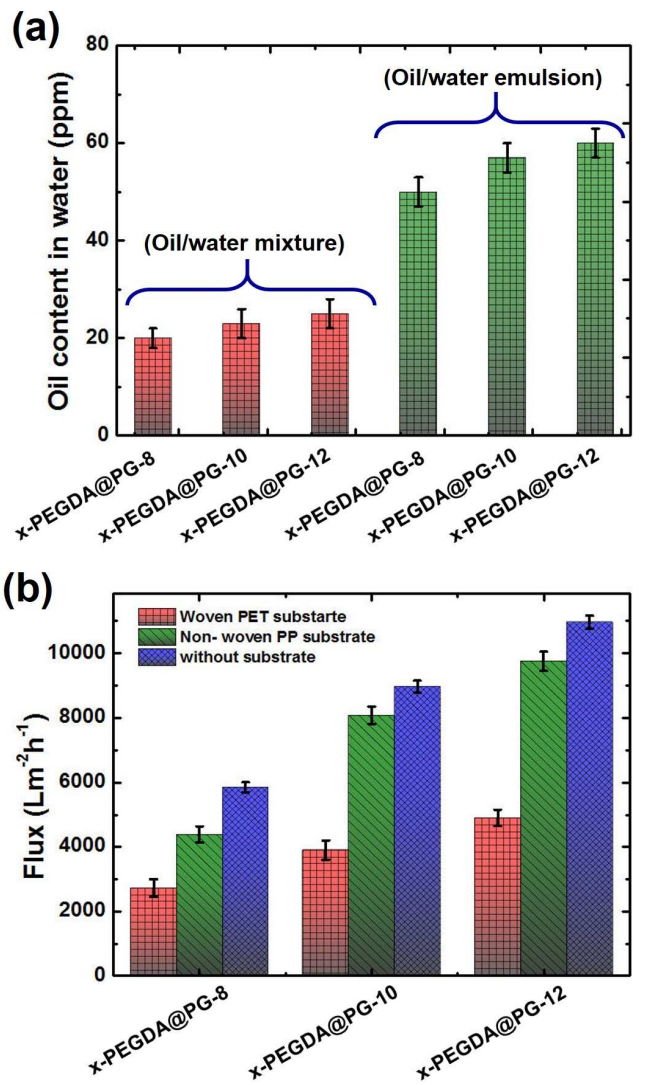

Fig. 7 Oil water separation results of various x-PEGDA@PG NF membranes. (a) Oil content in the filtrate after permeating oil/water mixture and oil in water emulsion through various x-PEGDA@PG-8, x-PEGDA@PG-10, and x-PEGDA@PG-12 NF membranes. (b) Flux for permeating oil/water mixture solely though x-PEGDA@PG-8, x-PEGDA@PG-10, and x-PEGDA@PG-12 NF membranes and also deposited on various substrates.

In case of highly porous membrane flow takes place through shorter and less tortuous path resulting in a smaller resistance or pressure drop with high permeability. The permeability of the membranes could also be measured by the mean flow pore diameter which revealed that the fifty percent of the flow is through pores larger than the mean flow pore diameter and the rest of the flow is through smaller pores. The mean flow pore diameter is obtained from the mean flow pressure yield a value of 1.48, 2.01, and 2.28 µm for x-PEGDA@PG-8, x-PEGDA@PG-10, and x-PEGDA@PG-12 NF membranes, respectively confirming the maximum permeability of x-PEGDA@PG-8 NF membrane. As per expectations, the as-prepared x-PEGDA@PG NF membranes, which combine the selective wettability and high porosity, have demonstrated efficient separation for both oil/water mixtures and oil-in-water emulsions. As a proof of concept, the solely gravity driven oil/water separation experiment was performed as shown in Fig. 5a. The x-PEGDA@PG-8 NF membrane was fixed at the middle of the device and a 200 mL of oil/water mixture (with a volume ratio of 150:50) were poured onto the upper glass tube. The water quickly passed through the prewetted superhydrophilic membranes and reached to the conical flask, and all of the oil was retained above the membrane due to the oleophobicity of the membranes. No external driven force was used during the fast separation process (within 100 sec). For further clearance, Fig 5b showed the images oil/water mixture as well as of corresponding oil and water after the separation. Over 149.5 mL water and 49.5 mL oil were collected, suggesting extremely high separation efficiency of the x-PEGDA@PG-8 NF membrane. More importantly, neither water nor oil is observed in collected oil or water, respectively, indicating a high purity and effectiveness of the separation of the oil/water mixture using the x-PEGDA@PG-8 NF membrane. For real time testing of the separation capability of the x-PEGDA@PG-8 NF membrane, a surfactant-stabilized (SDS) oil-in-water emulsion with a droplet size at the micrometer scale was prepared. 100 mL emulsion was poured onto the prewetted x-PEGDA@PG-8 NF membrane, water immediately permeated through the membrane and the emulsion droplets were demulsified upon touching to the membrane and the oil was retained above. Fig. 5c shows the optical microscopic images of original emulsion and the corresponding collected filtrate. Not a single droplet is observed in the collected filtrate, indicating the effectiveness of the x-PEGDA@PG-8 NF membrane for separating oil-in-water microemulsions.

For clear understanding of effective oil-in-water emulsion separation, a schematic has been presented in Fig. 6. Monodisperse oil-in-water emulsion with average diameter of oil droplets of 20 µm has been presented in Fig. 6a. The 5 µL droplet of oil-in-water emulsion using contact angle goniometer approaches to the surface of x-PEGDA@PG-8 NF membrane (Fig. 6b).

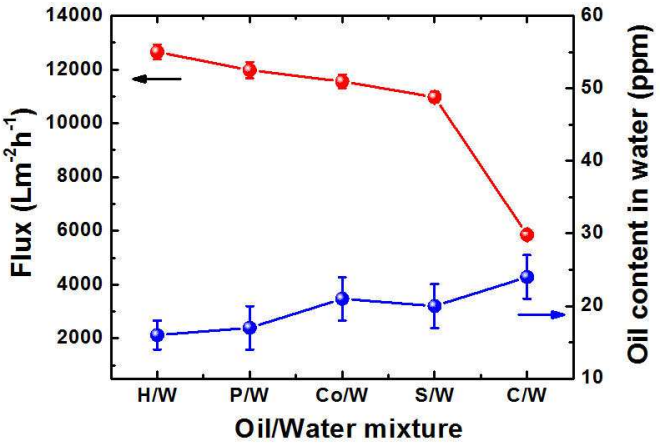

Fig. 8 Variation of flux and oil content in the filtrate as a function of permeated volume of the various oil/water mixture for x-PEGDA@PG-8 NF membrane.

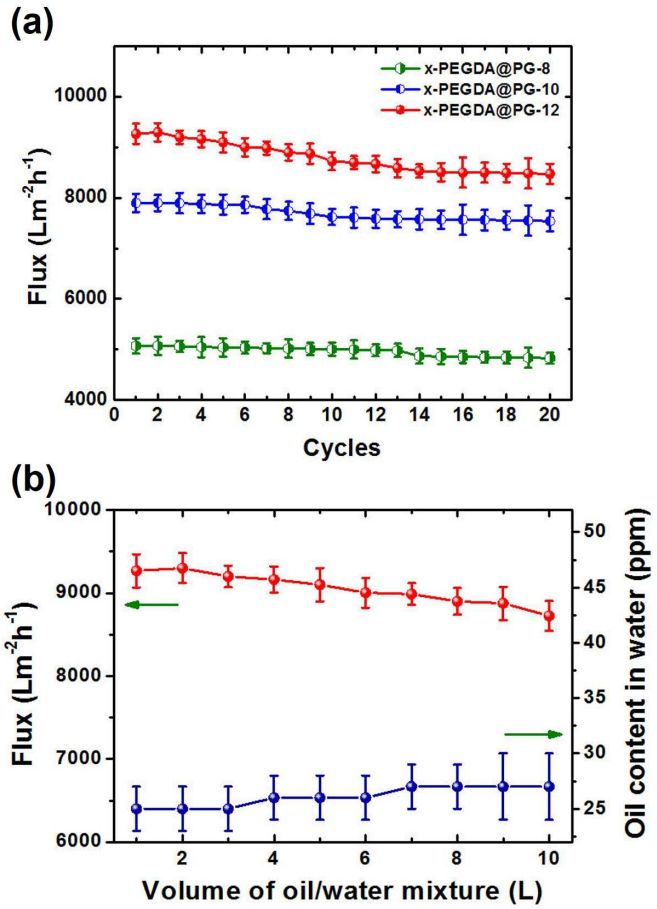

Fig. 9 (a) Real time monitoring of the flux with increasing cycle number using relevant x-PEGDA@PG-8, x-PEGDA@PG-10, and x-PEGDA@PG-12 NF membranes. (b) Variation of flux and oil content in the filtrate as a function of permeated volume of the oil/water mixture for x-PEGDA@PG-8 NF membrane.

Once the oil-in-water emulsion droplet contacts the x-PEGDA@PG-8 NF membrane surface, the measures contact angle was 45° at 0 s (Fig. 6c). Immediately after touching, the water phase in the form of droplets permeates into the x-PEGDA@PG-8 NF membrane pores leaving oil in the form of small droplets (Fig. 6d). Thus, exhibiting the satisfactory performance for separation of oil-in-water emulsion using x-PEGDA@PG-8 NF membrane.

For detailed investigation and for mass production, the largest size of membranes (60 × 60 cm) of x-PEGDA@PG NF membranes were facilely fabricated by using a 16 needles multi-jets electrospinning device (Fig. S5). It is quite possible to realize large scale industrial production by further enlarging the equipment. After that a series of oil/water mixtures as well as oil-in-water emulsions were poured onto the all types of NF membranes (x-PEGDA@PG-8, x-PEGDA@PG-10, and x-PEGDA@PG-12). Water immediately permeated through all these membrane and oil retained above and the oil content in water after only one separation was measured. As shown in Fig. 7a, for all types of NF membranes, the measured oil contents in the filtrate for oil/water mixture was below 26 ppm. Which is attributed to the presence of bigger oil droplets in the mixture that could not pass through the x-PEGDA@PG NF membranes. The oil content increases slightly from x-PEGDA@PG-8 to x-PEGDA@PG-12 NF membrane. This is the lowest value achieved by a NF membranes which is solely gravity-driven for oil/water separation reported so far. For oil-in-water emulsions, the residual oil contents were all about 60 ppm (higher values as compere to oil/water mixture separation), which might be due to the presence of extremely low sized few oil micro droplets. The water fluxes of NF membranes were also calculated by measuring the time for oil/water mixture of a certain volume to permeate through the specific area of the NF membrane. The measured fluxes of x-PEGDA@PG-8, x-PEGDA@PG-10, and x-PEGDA@PG-12 NF membranes without any substrate and also deposited on PET woven and PP non-woven has been presented in Fig. 7b. The highest fluxes of 4900, 9756, and 10975 L m^{-2} h^{-1} were achieved for PEGDA@PG-8, PEGDA@PG-10, and PEGDA@PG-12 NF membranes without using any substrate. Which was remarkably higher than that of commercial UF filtration membranes (usually with a flux of less than 300 L m^{-2} h^{-1}), and also form electrospun composite NF membrane (flux of less than 400-500 L m^{-2} h^{-1}).[10] As flux is the measurement of permeation of water through the membranes within the calculated time, thus the values of these remarkable flux rates of as-prepared NF membranes is the clear indication of ultrafast oil/water separation with respect to the pore size of the membranes. Although, nanowire haired meshes have also shown very high flux of 127 000 L m^{-2} h^{-1}, but the mean pore size (64 µm) of working membranes were also very high, and if the pore size was reduced to 1 µm, the flux have also shown great decline to 500 L m^{-2} h^{-1}.[55] So our membranes with mean pore size in the range of 1.4-2.4 µm have given maximum values of fluxes reported so far. Additionally we have also measured the flux rates of oil/water mixtures using various densities of oils, as shown in Fig. 8. For H/W, P/W, Co/W, and S/W we got the comparable values of fluxes of 12656, 11976, 11565, and 10975 L m^{-2} h^{-1}, because the densities of all types of oils lie in the range of 650-926 Kg m^3 (Low density oils). On contrary, we observed a decline of flux using C/W mixture (5853 L m^{-2} h^{-1}) due to high density of oil, which make a barrier layer at the top of membrane and thus reduced the permeability of water. The oil content in the permeate was also presented in Fig. 8, which lie in the range of 16-24 ppm. So our membranes are suitable for variety of oil/water mixture separation.

Moreover, the antifouling performance presented in Fig. 9a indicated the outstanding reusability of the NF membranes, with nearly no flux decrease after 10 cycles and very minute decrease in flux after 20 cycles for all types of NF membranes. For antifouling performance, water was passed through the membrane and simultaneously oil accumulated above the membrane was continuously removed to avoid the blocking of water permeation. Continuous separation of an oil water mixture up to 10 L was achieved by using a x-PEGDA@PG-8 NF membrane as shown in Fig. 9b. During the whole testing process, very minute flux decrease occurred and the oil content

in the filtrate remains around 25 ppm. This result indicated the capability of the membrane for treating a large amount of an oil/water mixture and a superior antifouling property for long time usage.

Conclusions

In summary, we have demonstrated a facile approach for fabricating superhydrophilic and prewetted oleophobic nanofibrous membranes that allow effective separation of both water rich immiscible and monodispersed oil/water mixtures with extremely high separation efficiency and separation capacity. The *in situ* cross-linked x-PEGDA@PG NF membranes have shown superhydrophilicity with ultralow time of wetting and promising oleophobicity (OCA = 105°). Solely driven by gravity, x-PEGDA@PG NF membranes with mean pore size between 1.5-2.6 μm have shown very high flux rate of 10,975 L m^{-2} h^{-1} which was much larger than those of commercial filtration membranes with similar permeation properties. More importantly, the membrane exhibits good separation efficiency (residual oil content in the filtrate is 26 ppm) as well high separation capacity, which can separate 10 L of an oil/water mixture continuously without a decline in flux and excellent antifouling property for long term use. Thus making them an important candidate for treating real emulsified wastewater on a mass scale and for crude oil purification especially for high viscosity oil purification.

Acknowledgements

This work is supported by the National Natural Science Foundation of China (No. 51322304), the Fundamental Research Funds for the Central Universities, and the "DHU Distinguished Young Professor Program" and Deanship of Scientific Research at King Saud University (No. RGP-VPP-089).

Notes and references

[a] State Key Laboratory for Modification of Chemical Fibers and Polymer Materials, College of Materials Science and Engineering, Donghua University, Shanghai 201620, China. E-mail: binding@dhu.edu.cn
[b] Nanomaterials Research Centre, Modern Textile Institute, Donghua University, Shanghai 200051, China
[c] Petrochemical Research Chair, Department of Chemistry, College of Science, King Saud University, Riyadh 11451, Saudi Arabia. E-mail: ssdeyab@ksu.edu.sa
[d] Department of Chemistry, Faculty of Science, Tanta University, Tanta 31527, Egypt
Electronic Supplementary Information (ESI) available: [details of any supplementary information available should be included here]. See DOI: 10.1039/b000000x/

1. Y. Yang, H. Wang, J. Li, B. He, T. Wang and S. Liao, *Environ. Sci. Technol.*, 2012, **46**, 6815-6821.
2. T. Sakthivel, D. L. Reid, I. Goldstein, L. Hench and S. Seal, *Environ. Sci. Technol.*, 2013, **47**, 5843-5850.
3. J. H. Vandermeulen and C. W. Ross, *J. Environ. Manage.*, 1995, **44**, 297-308.
4. R. Margesin and F. Schinner, *J. Chem. Technol. Biot.*, 1999, **74**, 381-389.
5. J. V. Mullin and M. A. Champ, *Spill Sci. Technol. B*, 2003, **8**, 323-330.
6. A. Zolfaghari-Baghbaderani, M. Emtyazjoo, P. Poursafa, S. Mehrabian, S. Bijani, D. Farkhani and P. Mirmoghtadaee, *J. Environ. Public Health*, 2012, **2012**, 981365-981365.
7. A. B. Nordvik, J. L. Simmons, K. R. Bitting, A. Lewis and T. StromKristiansen, *Spill Sci. Technol. B*, 1996, **3**, 107-122.
8. R. Mohammadi, J. Wassink and A. Amirfazli, *Langmuir*, 2004, **20**, 9657-9662.
9. Y. Shang, Y. Si, A. Raza, L. Yang, X. Mao, B. Ding and J. Yu, *Nanoscale*, 2012, **4**, 7847-7854.
10. W. Zhang, Z. Shi, F. Zhang, X. Liu, J. Jin and L. Jiang, *Adv. Mater.*, 2013, **25**, 2071-2076.
11. A. Raza, Y. Si, X. Wang, T. Ren, B. Ding, J. Yu and S. S. Al-Deyab, *Rsc Adv.*, 2012, **2**, 12804-12811.
12. H. Ma, C. Burger, B. S. Hsiao and B. Chu, *Biomacromolecules*, 2011, **12**, 970-976.
13. H. Ma, K. Yoon, L. Rong, Y. Mao, Z. Mo, D. Fang, Z. Hollander, J. Gaiteri, B. S. Hsiao and B. Chu, *J. Mater. Chem.*, 2010, **20**, 4692-4704.
14. X. Wang, K. Zhang, Y. Yang, L. Wang, Z. Zhou, M. Zhu, B. S. Hsiao and B. Chu, *J. Membrane Sci.*, 2010, **356**, 110-116.
15. J. Lin, F. Tian, Y. Shang, F. Wang, B. Ding and J. Yu, *Nanoscale*, 2012, **4**, 5316-5320.
16. J. Wu, N. Wang, L. Wang, H. Dong, Y. Zhao and L. Jiang, *ACS Appl. Mater. Interfaces*, 2012, **4**, 3207-3212.
17. J. Lin, F. Tian, Y. Shang, F. Wang, B. Ding, J. Yu and Z. Guo, *Nanoscale*, 2013, **5**, 2745-2755.
18. X. Tang, Y. Si, J. Ge, B. Ding, L. Liu, G. Zheng, W. Luo and J. Yu, *Nanoscale*, 2013, **5**, 11657-11664.
19. X. Zhongxin, L. Mingjie and J. Lei, *J. Polym. Sci. Pol. Phys.*, 2012, **50**, 5-20.
20. B. Simoncic, B. Tomsic, L. Cerne, B. Orel, I. Jerman, J. Kovac, M. Zerjav and A. Simoncic, *J. Sol-Gel Sci. Techn.*, 2012, **61**, 340-354.
21. D. Han and A. J. Steckl, *Langmuir*, 2009, **25**, 9454-9462.
22. F. Likibi, B. Jiang and B. Li, *J. Mater. Res.*, 2008, **23**, 3222-3228.
23. L. Xiaoxuan, W. Guangguo, L. Yuanpei and M. Han, *J. Membrane Sci.*, 2006, **283**, 13-20.
24. M. Jin, J. Wang, X. Yao, M. Liao, Y. Zhao and L. Jiang, *Adv. Mater.*, 2011, **23**, 2861-2864.
25. Y. C. Jung and B. Bhushan, *Langmuir*, 2009, **25**, 14165-14173.
26. M. A. Kanjwal, N. A. M. Barakat, F. A. Sheikh, G. G. Kumar, D. K. Park and H. Y. Kim, *J. Ceram. Process. Res.*, 2010, **11**, 437-442.
27. X. Wang, B. Ding, G. Sun, M. Wang and J. Yu, *Prog. Mater. Sci.*, 2013, **58**, 1173-1243.
28. B. Ding, M. Wang, X. Wang, J. Yu and G. Sun, *Materials Today*, 2010, **13**, 16-27.
29. X. Wang, B. Ding, J. Yu and M. Wang, *Nano Today*, 2011, **6**, 510-530.
30. J. Lin, X. Wang, B. Ding, J. Yu, G. Sun and M. Wang, *Cr. Rev. Sol. State*, 2012, **37**, 94-114.
31. M. Swart and P. E. Mallon, *Pure App. Chem.*, 2009, **81**, 495-511.

32. V. A. Ganesh, H. K. Raut, A. S. Nair and S. Ramakrishna, *J. Mater. Chem.*, 2011, **21**, 16304-16322.
33. J. Wang, A. Raza, Y. Si, L. Cui, J. Ge, B. Ding and J. Yu, *Nanoscale*, 2012, **4**, 7549-7556.
34. J. Lin, Y. Shang, B. Ding, J. Yang, J. Yu and S. S. Al-Deyab, *Mar. Pollut. Bull.*, 2012, **64**, 347-352.
35. J. Lin, B. Ding, J. Yang, J. Yu and G. Sun, *Nanoscale*, 2012, **4**, 176-182.
36. J. Lin, B. Ding, J. Yang, J. Yu and S. S. Al-Deyab, *Mater. Lett,*, 2012, **69**, 82-85.
37. J. Du, J. Dai, J. L. Liu and T. Dankovich, *React. Funct. Polym.*, 2006, **66**, 1055-1061.
38. X. Liu, J. Zhou, Z. Xue, J. Gao, J. Meng, S. Wang and L. Jiang, *Adv. Mater.*, 2012, **24**, 3401-3405.
39. Q. Cheng, M. Li, Y. Zheng, B. Su, S. Wang and L. Jiang, *Soft Matter*, 2011, **7**, 5948-5951.
40. M. Sun, X. Li, B. Ding, J. Yu and G. Sun, *J. Colloid. Interf. Sci.*, 2010, **347**, 147-152.
41. K. H. Lee, H. Y. Kim, Y. J. Ryu, K. W. Kim and S. W. Choi, *J. Polym. Sci. Pol. Phys.*, 2003, **41**, 1256-1262.
42. K. Lee, B. Lee, C. Kim, H. Kim, K. Kim and C. Nah, *Macromol Res*, 2005, **13**, 441-445.
43. F. Zhao, X. Wang, B. Ding, J. Lin, J. Hu, Y. Si, J. Yu and G. Sun, *Rsc Adv.*, 2011, **1**, 1482-1488.
44. L. Yang, A. Raza, Y. Si, X. Mao, Y. Shang, B. Ding, J. Yu and S. S. Al-Deyab, *Nanoscale*, 2012, **4**, 6581-6587.
45. Y. Zhou, X. Fan, D. Xue, J. Xing and J. Kong, *React. Funct. Polym.*, 2013, **73**, 508-517.
46. K. Nalampang, R. Panjakha, R. Molloy and B. J. Tighe, *J. Biomat. Sci-Polym. E.*, 2013, **24**, 1291-1304.
47. A. Fathi, S. Lee, X. Zhong, N. Hon, P. Valtchev and F. Dehghani, *Polymer*, 2013, **54**, 5534-5542.
48. Q. Wang, L. Ren, Y. Wang, Y. Yao and S. Hou, *J. South China Uni. Tech. Nat. Sci. E.*, 2013, **41**, 62-67.
49. G. McHale, N. J. Shirtcliffe and M. I. Newton, *Langmuir*, 2004, **20**, 10146-10149.
50. B. Emami, H. V. Tafreshi, M. Gad-el-Hak and G. C. Tepper, *J. App. Phys.*, 2012, **111**.
51. A. Raza, Y. Si, B. Ding, J. Yu and G. Sun, *J. Colloid. Interf. Sci.*, 2013, **395**, 256-262.
52. V. Hejazi, A. E. Nyong, P. K. Rohatgi and M. Nosonovsky, *Adv. Mater.*, 2012, **24**, 5963-5966.
53. Y. Si, T. Ren, B. Ding, J. Yu and G. Sun, *J. Mater. Chem.*, 2012, **22**, 4619-4622.
54. Y. Si, T. Ren, Y. Li, B. Ding and J. Yu, *Carbon*, 2012, **50**, 5176-5185.
55. F. Zhang, W. B. Zhang, Z. Shi, D. Wang, J. Jin and L. Jiang, *Adv. Mater.*, 2013, **25**, 4192-4198.